

# Low-Threshold Strained Quantum-Well GaSb-Based Lasers Emitting in the 2.5- to 2.7- $\mu\text{m}$ Wavelength Range

Kaveh Kashani-Shirazi, Kristijonas Vizbaras, Alexander Bachmann, *Student Member, IEEE*, Shamsul Arafin, and Markus-Christian Amann, *Fellow, IEEE*

**Abstract**—GaInAsSb–GaSb strained quantum-well (QW) ridge waveguide diode lasers emitting in the wavelength range from 2.51 to 2.72  $\mu\text{m}$  have been grown by molecular beam epitaxy. The devices show ultralow threshold current densities of 44  $\text{A}/\text{cm}^2$  ( $L \rightarrow \infty$ ) for a single QW device at 2.51  $\mu\text{m}$ , which is the lowest reported value in continuous-wave operation near room temperature (15 °C) at this wavelength. The devices have an internal loss of 3  $\text{cm}^{-1}$  and a characteristic temperature of 42 K. By using broader QWs, wavelengths up to 2.72  $\mu\text{m}$  could be achieved.

**Index Terms**—Optical spectroscopy, quantum-well (QW) lasers.

## I. INTRODUCTION

GALLIUM ANTIMONIDE (GaSb) lasers are ideal light sources for tunable diode laser absorption spectroscopy [1], as they can access the midinfrared wavelength region between 2 and 4  $\mu\text{m}$ . In this range, many technologically important gases such as CO show strong absorption lines [2]. With increasing wavelength, several problems occur. Internal losses, such as intravalence band absorption, increase strongly and Auger recombination becomes a significant carrier loss mechanism [3]. In order to lower the transition energy, one increases the indium concentration of the GaInAsSb quantum wells (QWs) and, to compensate the resulting strain, also the arsenic content. This brings the alloy deeper in the miscibility gap and makes it more difficult to grow [4]. However, the high In content leads to very low valence band offsets and, when using GaSb as a barrier material, to a type-II-alignment with In concentrations of more than about 45%. In the past, AlGaAsSb with Al contents ranging from 25% to 40% was used as a barrier material to avoid this problem [5]. To achieve room-temperature continuous-wave (CW) operation, 2.7- $\mu\text{m}$  GaSb-based lasers, Al<sub>0.30</sub>Ga<sub>0.70</sub>As<sub>0.03</sub>Sb<sub>0.97</sub> barrier was used by Garbuzov *et al.* [6]. But this leads to very high conduction band offsets of more than 500 meV, which can result in inhomogeneous filling of a multiple QW structure. At 2.7  $\mu\text{m}$ , the best recorded

Manuscript received March 30, 2009; revised April 23, 2009. First published June 02, 2009; current version published July 24, 2009. This work was supported by the European Union under NEMIS (Contract FP6-2005-IST-5-031845) and by the German Federal Ministry of Education and Research under NOSE (Contract 13N8772).

The authors are with the Walter Schottky Institut, Technische Universität München, 85748 Garching, Germany (e-mail: Kashani@wsi.tum.de; Kristijonas.vizbaras@wsi.tum.de; bachmann@wsi.tum.de; arafin@wsi.tum.de; amann@wsi.tum.de).

Digital Object Identifier 10.1109/LPT.2009.2023077

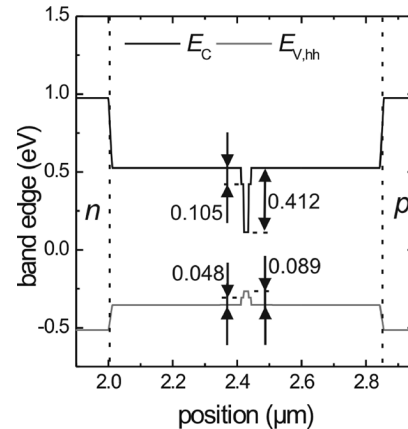


Fig. 1. Schematic energy band diagram of the 2.51- $\mu\text{m}$  RWG laser with band offsets given in electronvolts.

values for the threshold current density are 350  $\text{A}/\text{cm}^2$  for 2-mm-long devices [7]. Lin *et al.* presented devices at 2.73  $\mu\text{m}$  with 79- $\text{A}/\text{cm}^2$  threshold current density per QW (extrapolated to infinite length:  $L \rightarrow \infty$ ) in pulsed operation [5]. In this letter, we present three different ridge waveguide (RWG) lasers with varying QW thicknesses emitting CW at room temperature between 2.51 and 2.72  $\mu\text{m}$ , showing ultralow threshold current densities.

## II. DEVICE FABRICATION

### A. Design and Epitaxy

The structures were grown on an n-type GaSb substrate. The growth starts with a 2- $\mu\text{m}$ -thick cladding layer of Al<sub>0.50</sub>Ga<sub>0.50</sub>As<sub>0.04</sub>Sb<sub>0.96</sub> with a Te doping of  $2 \cdot 10^{18} \text{ cm}^{-3}$  followed by a 400-nm nominally undoped Al<sub>0.10</sub>Ga<sub>0.90</sub>As<sub>0.01</sub>Sb<sub>0.99</sub> waveguide layer, which also serves as a separate confinement layer. Next, the active region with Ga<sub>0.57</sub>In<sub>0.43</sub>As<sub>0.14</sub>Sb<sub>0.86</sub> QWs between GaSb barriers is deposited. One 10-nm QW and one 15-nm QW are used for the shorter wavelength devices at 2.51 and 2.65  $\mu\text{m}$ , respectively. The 2.72- $\mu\text{m}$  device holds two 20-nm QWs with a GaSb barrier of 8 nm between the wells. The p-side is equivalent to the n-side but with a Si doping of  $5 \cdot 10^{17} \text{ cm}^{-3}$  in the cladding and is followed by a highly p-doped GaSb contact layer. The QWs are 1.7% compressively strained. A band structure of the device, calculated with nextnano<sup>++</sup> [8] with material parameters taken from [9], can be seen in Fig. 1. The figure also shows the band

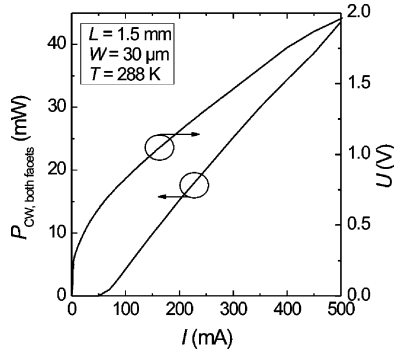


Fig. 2. Power versus current and voltage versus current characteristics of a  $L = 1.5$  mm long and  $W = 30$   $\mu\text{m}$  wide RWG laser at  $2.51$   $\mu\text{m}$  at  $T = 288$  K.

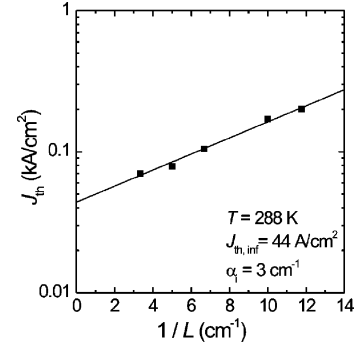


Fig. 3. CW threshold current densities versus inverse length of the  $2.51$ - $\mu\text{m}$  RWG laser at  $T = 288$  K. The extrapolated current density at infinite length is  $J_{\text{th,inf}} = 44$   $\text{A}/\text{cm}^2$  and the internal losses are  $\alpha_i = 3$   $\text{cm}^{-1}$ .

offsets between the waveguide, barrier, and QW layers (no quantization included). The relatively low Al content in the cladding and waveguide layers still leads to a relatively high optical confinement in the active region ( $\Gamma_{\text{QW}} = 2 \times 2.7\%$ ,  $\Gamma_{\text{Cl}} = 2 \times 10.0\%$  for the  $2.7$   $\mu\text{m}$  device) and to low absorption losses in the doped cladding layers. It was chosen to keep the growth temperature as low as possible since materials with higher Al contents can only be grown in good quality at elevated temperatures ( $>500$   $^{\circ}\text{C}$ ). In our structure, the active region and the layers following it were grown at  $430$   $^{\circ}\text{C}$  to avoid a deterioration of the active region due to *in situ* annealing during the growth of the upper cladding [10]. All samples were grown on a Varian Gen-II-MBE system with solid sources and valved cracker cells for arsenic and antimony.

### B. Processing and Measurement

RWG lasers with stripe widths ranging from  $15$  to  $200$   $\mu\text{m}$  were processed by dry chemical etching of the cladding and part of the waveguide layer,  $\text{SiO}_2$ -passivation and deposition of Ti–Pt–Au contacts on the top and bottom. The structures were cleaved at different lengths and mounted epi-side up on copper heat sinks. The lasers are not equipped with a facet coating. All measurements were taken at  $15$   $^{\circ}\text{C}$  on a temperature-controlled heat sink.

## III. RESULTS

The devices with the  $10$ -nm QW emit at  $2.51$   $\mu\text{m}$ . The power versus current and voltage versus current characteristics of a  $1.5$ -mm-long and  $30$ - $\mu\text{m}$ -wide device at room temperature are shown in Fig. 2. The maximum output power of  $44$  mW (for both facets) is limited by the current source. Internal losses are calculated to  $3$   $\text{cm}^{-1}$ . The characteristic temperature was measured with  $500$ -ns-wide pulses at  $200$ -Hz repetition rate and was found to be  $42$  K and the differential quantum (per face) is  $11\%$ .

The CW threshold current densities of several devices with varying length are shown in Fig. 3. The effect of lateral diffusion and drift of the carriers on the measured current density have been considered by taking

$$J_{\text{th}}(w) = J_{\text{th}} \cdot \left(1 + \frac{\Delta w}{w}\right) \quad (1)$$

TABLE I  
DEVICE PROPERTIES

$d_{\text{QW}}$ (nm)	$\lambda$ ( $\mu\text{m}$ )	$J_{\text{th,inf}}$ ( $\text{A}/\text{cm}^2$ )	$T_0$ (K)
10	2.51	44 (1 QW)	42
15	2.65	50 (1 QW)	62
20	2.72	87 (2 QWs)	65

Device properties of the GaInAsSb–GaSb lasers for CW operation at  $288$  K with  $d_{\text{QW}}$  as the QW width,  $\lambda$  as the emission wavelength,  $J_{\text{th,inf}}$  as the extrapolated threshold current density length, and  $T_0$  as the characteristic temperature.

where  $w$  and  $\Delta w$  denote stripe width and the lateral broadening on both sides for a given laser length.  $J_{\text{th}}(w)$  and  $J_{\text{th}}$  are the threshold current densities for stripe width  $w$  and for infinite stripe width, respectively. From the  $w$ -dependence of the threshold current densities, a value of  $4.2$   $\mu\text{m}$  was found for the lateral broadening  $\Delta w$ .

The extrapolated current density for an infinitely long device is  $44$   $\text{A}/\text{cm}^2$ . The lowest measured value is  $70$   $\text{A}/\text{cm}^2$  for a  $3$ -mm-long device. The  $2.73$ - $\mu\text{m}$  device shows a measured threshold current density per QW of  $70$   $\text{A}/\text{cm}^2$  for a  $2$ -mm-long device, which is by a factor of  $5$  better than presented in [7].

As can be seen in Table I, all devices show extremely low threshold current densities. This can be attributed to the improved design with low optical losses, good carrier confinement in the active region, and excellent material quality. The threshold current density rises with increasing wavelength due to lower optical confinement in the active region and higher losses (Auger, optical losses). Note that the  $2.72$ - $\mu\text{m}$  device has two QWs. This device shows better threshold current density *per QW* compared to the devices with only one QW as each well needs lower gain at threshold to compensate for the total optical losses in the device.

The different emission wavelengths are due to the effect of the quantization in the narrow QWs, which accounts for  $60$  meV in the  $10$ -nm and  $23$  meV in the  $20$ -nm well. For long wavelength devices, where the transition energy is in the range of  $400$ – $500$  meV, the quantization energy is a particularly important contribution. Alternatively, one can add more In to the QW material to reach the desired wavelength. Diode lasers with  $7$ -nm-wide  $\text{Ga}_{0.50}\text{In}_{0.50}\text{As}_{0.14}\text{Sb}_{0.86}$  QWs were grown and processed the same way as the other presented devices

but the devices showed no CW lasing at room temperature. We assume that the inferior properties are due to the vanishing valence band offset and lower conduction band offset.

The temperature behavior of GaInAsSb-based lasers tends to deteriorate strongly with increasing wavelength [6]. Although the devices with wide QWs show the longest emission wavelength, the characteristic temperature is best for this structure. This behavior is not fully understood. Possible reasons are less interface recombination in wide QWs, decreased thermionic emissions of carriers due to higher offsets between barrier conduction band and quantized level energy in the wells, or a decrease of Auger recombination losses.

#### IV. CONCLUSION

In summary, we have demonstrated ultralow threshold edge emitters in the 2.51- to 2.72- $\mu\text{m}$  wavelength range. A value of 44 A/cm<sup>2</sup> is the smallest threshold current density reported so far for any diode laser emitting CW at room temperature in this wavelength range. The performance of the devices is comparable to the well-known InP and GaAs material system. Aiming for longer wavelengths, a comparison of different QW widths shows that using thick QWs is preferable to increasing the In content of the QW.

#### REFERENCES

- [1] A. Vicet, D. A. Yarekha, A. Pérona, Y. Rouillard, S. Gaillard, and A. N. Baranov, "Trace gas detection with antimonide-based quantum-well diode lasers," *Spectrochimica Acta.*, vol. 58, pt. A, pp. 2405–2412, 2002.
- [2] L. Rothman, "The HITRAN 2004 molecular spectroscopic database," *J. Quant. Spectrosc. Radiat. Transf.*, vol. 96, pp. 139–204, 2005.
- [3] A. Chandola, R. Pino, and P. S. Dutta, "Below bandgap optical absorption in tellurium-doped GaSb," *Semicond. Sci. Technol.*, vol. 20, no. 8, pp. 886–893, 2005.
- [4] V. Sorokin, S. Sorokin, A. Semenov, B. Meltser, and S. Ivanov, "Novel approach to the calculation of instability regions in GaInAsSb alloys," *J. Cryst. Growth*, vol. 216, pp. 97–103, 2000.
- [5] C. Lin, M. Grau, O. Dier, and M.-C. Amann, "Low threshold room-temperature continuous-wave operation of 2.24–3.04  $\mu\text{m}$  GaInAsSb/AlGaAsSb quantum-well lasers," *Appl. Phys. Lett.*, vol. 84, pp. 5088–5090, 2004.
- [6] D. Z. Garbuzov, H. Lee, V. Khalfin, R. Martinelli, J. C. Connolly, and G. L. Belenky, "2.3–2.7- $\mu\text{m}$  room temperature CW operation of InGaAsSb–AlGaAsSb broad waveguide SCH-QW diode lasers," *IEEE Photon. Technol. Lett.*, vol. 11, no. 7, pp. 794–796, Jul. 1999.
- [7] J. G. Kim, L. Shterengas, R. U. Martinelli, and G. L. Belenky, "High-power room-temperature continuous wave operation of 2.7 and 2.8  $\mu\text{m}$  In(Al)GaAsSb/GaSb diode lasers," *Appl. Phys. Lett.*, vol. 83, pp. 1926–1928, 2003.
- [8] *For Obtaining the Nextnano Executables and Related Publications*, [Online]. Available: <http://www.wsi.tum.de/nextnano>
- [9] I. Vurgaftman, J. R. Meyer, and L. R. Ram-Mohan, *J. Appl. Phys.*, vol. 89, pp. 5815–5875, 2001.
- [10] O. Dier, S. Dachs, M. Grau, C. Lin, C. Lauer, and M.-C. Amann, "Blue shift of the photoluminescence of GaInAsSb caused by thermal annealing," *Appl. Phys. Lett.*, vol. 86, pp. 151120-1–151120-3, 2005.